Seismic anisotropy in the lower mantle: A comparison of waveform splitting of SKS and SKKS

Fenglin Niu and Anisa M. Perez

Department of Earth Science, Rice University, Houston, Texas, USA

Received 4 August 2004; revised 16 October 2004; accepted 30 November 2004; published 28 December 2004.

[1] We have carried out a global investigation on seismic anisotropy in the lower mantle by comparing the waveform splitting of *SKS* and *SKKS* found at the same seismogram. The two shear waves have very similar ray paths in the upper mantle but different ones in the lower mantle. We collected a total of 104 *SKS*+*SKKS* waveform data recorded at 76 stations. The *SKS*+*SKKS* data are first matched with a single anisotropic model (2 parameters: the fast polarization direction φ and delay time δt) and two independent anisotropic models (4 parameters). We then applied an *F-test* to examine whether the 4-parameter models are better than the 2-parameter ones based on error improvement. We found that the data from most of the stations can be explained by the simple 2-parameter models. While this observation provides compelling evidence that the vast part of the lower mantle below ~1000 km (including the D'' region) is transversely isotropic, it is still arguable that the uppermost lower mantle and the transition may partly contribute the *SKS*/*SKKS* splittings. We also found that the 4-parameter models provide a better fitting to the *SKS* and *SKKS* splitting at 8 stations, suggesting the existence of transverse anisotropy or anomalous dipping structures in some part of the lower mantle. *INDEX TERMS:* 3902 Mineral Physics: Creep and deformation; 3909 Mineral Physics: Elasticity and anelasticity; 7203 Seismology: Body wave propagation; 7205 Seismology: Continental crust (1242); 7260 Seismology: Theory and modeling. **Citation:** Niu, F., and A. M. Perez (2004), Seismic anisotropy in the lower mantle: A comparison of waveform splitting of SKS and SKKS, *Geophys. Res. Lett.*, *31*, L24612, doi:10.1029/2004GL021196.

1. Introduction

[2] Numerous seismic observations have shown that the earth's upper mantle exhibit anisotropy for seismic wave propagation [e.g., *Silver*, 1996]. This seismic anisotropy is well explained by two facts observed from upper mantle minerals. These minerals are microscopically anisotropic; both compressional and shear waves vary significantly along different orientations of the crystal lattice. Aggregates of these minerals could develop strong fabric when experienced anelastic deformations, for example, associated with mantle flow [e.g., *Nicolas and Christensen*, 1987]. For those reasons, seismic anisotropy has been widely used to understand the deformation associated with various mantle processes [*Silver and Chan*, 1991; *Vinnik et al.*, 1992].

[3] Shear-wave splitting is the most unambiguous manifestation of anisotropy. Splitting measurements (the fast polarization direction, φ, and delay time, δt, between the fast and slow directions) of shear waves, mostly the core phases such as *SKS* and *SKKS*, are now made routinely and used to study upper mantle anisotropy. Because of the *P-to-S* conversion at the core-mantle boundary (CMB), the observed anisotropy can be confined within the mantle along the receiver-side path. Also these *P-to-S* conversion phases are expected to be radially polarized in an isotropic and spherically symmetric earth, any detectable energy on the transverse component (T-component) can be attributed to anisotropy. This simplicity allows for robust measurements of anisotropy.

[4] Splittings of the *SKS*/*SKKS* waves result from the anisotropy accumulated along the entire ray path from the CMB to the receiver (Figure 1). Yet, the origin of the observed splittings is usually assumed to be the upper mantle anisotropy formed by tectonic processes [*Silver*, 1996]. There are several arguments for this assumption based on both seismological and laboratory observations [e.g., *Meade et al.*, 1995]. *SKS* waves from different earthquakes with various back azimuths recorded at a single station, which have close ray paths in the upper mantle and very different ones in the lower mantle, are usually found to have nearly similar splitting patterns [*Silver and Chan*, 1991]. Different types of S waves, for example, *S* and *ScS* from deep earthquakes, no matter whether or not they traverse through the low mantle, appear to show almost identical splittings [*Meade et al.*, 1995]. Although both experimental and theoretical studies indicate that the lower mantle mineral phases, such as the orthorhombic-structured $MgSiO_3$ perovskite, exhibit strong single crystal anisotropy at both ambient and high pressure and temperature conditions [*Yeganeh-Haeri*, 1994; *Mainprice et al.*, 2000], the aggregates of these minerals, on the other hands, do not show any significant preferred orientation at high pressure and low temperature condition [e.g., *Meade et al.*, 1995].

[5] Recent laboratory study by *Cordier et al.* [2004], however, shows that dislocation creep occurs in $MgSiO_3$ perovskite at pressure-temperature conditions equivalent to the uppermost lower mantle, which may explain the seismic observation by *Wookey et al.* [2002], who found some degree of seismic anisotropy at mid-mantle depths. It also should be noticed that employing a comparison of *ScS* and *SKS* might be improper to infer lower mantle anisotropy since *ScS* splitting could be affected by source-side anisotropy even intermediate-depth or deep earthquakes are used. Anisotropy within subducting slabs could be strongly heterogeneous and complicated [*Hiramatsu et al.*, 1997]. The ideal pair of seismic waves for identifying lower mantle anisotropy is *SKS vs. P660s* [*Vinnik and Montagner*, 1996; *Iidaka and Niu*, 1998]. The later travels most of the path as a P wave and converts to S wave at the 660-km discontinuity

0094-8276/04/2004GL021196$05.00

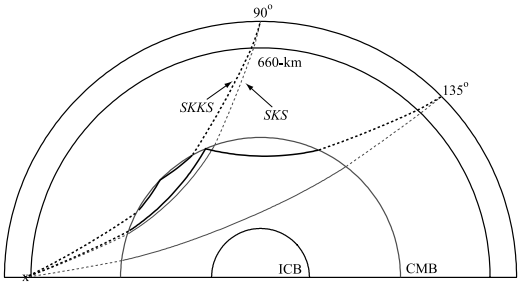

Figure 1. *SKS* and *SKKS* ray paths at the distances of 90–135° based on *iasp91* [*Kennett and Engdahl*, 1991]. P- and S-wave ray segments are shown by solid and dashed lines, respectively. Note that the two have almost identical ray paths in the upper mantle. Thus similar splitting behavior is expected if the lower mantle is isotropic.

beneath the station. At a distance of ~85°, the two have an almost identical S-wave path in the upper mantle, but an S- and P-wave ray segment in the lower mantle, respectively (see their Figure 1). *Iidaka and Niu* [1998] observed a difference of ~0.4 s in splitting time between the two phases and interpreted it as possible anisotropy in the lower mantle, either the D'' or any other regions. The lower amplitude of the *P660s* is the drawback of this method, which could introduce large uncertainty in splitting measurement.

[6] Another well-used method for looking up lower mantle anisotropy is to compare *SKS* splitting using earthquakes from different back azimuths. However, because of the uneven distribution of seismicity, it is quite often that robust measurements from two nonorthogonal back azimuths are not available. Moreover, even if *SKS* splitting shows a dependence on back azimuth, it may be caused by a vertically varying anisotropy in the upper mantle instead of the lower mantle [e.g., *Silver and Savage*, 1994; *Rumpker and Silver*, 1998], as well as receiver-side scattering. In this study, we employed a different way to investigate the issue by comparing splitting of *SKS* and *SKKS* with comparable amplitude found at a seismogram. The two have very similar ray paths in the upper mantle, but different ones in the lower mantle. Furthermore, they have the same back azimuth, it is thus not necessary to consider the effect of multiple anisotropic layers. Consequently any difference in splitting between the two indicates the presence of seismic anisotropy or dipping structures in the lower mantle. Since *SKS* and *SKKS* are indistinguishably used in measuring the upper mantle anisotropy to increase azimuth coverage, a systematic comparison of the splitting behavior of the two is also essential to the justification of the usage.

2. A Global *SKS*+*SKKS* Dataset

[7] The *SKS*+*SKKS* data are collected from the seismic data recorded by IRIS Global Seismographic Network (GSN) and other PASSCAL stations in the period of 1990–2003. Only intermediate-depth and deep earthquakes are used to ensure the quality of data. More than ten thousands of seismograms are visually checked and a total of 104 *SKS*/*SKKS* pairs are finally selected. Epicentral distance ranges from ~95° to ~135°. The dataset has a relatively good coverage of the globe, with 76 stations and 90 events (Figure 2). We chose the data based on the following criteria: (1) both phases are clear shown on the radial component. A signal-to-noise ratio (SNR) ≥ 3 is used for both SKS_R and $SKKS_R$. (2) Amplitude of SKS_R and $SKKS_R$ are comparable with each other. We limited the amplitude ratio $SKKS_R/SKS_R$ to the range of 0.5–2. This ensures us to obtain similar precisions of the two in splitting measurement; (3) there are no other phases, such as the depth phase of *SKS*, arrive at the time window of *SKKS*.

[8] Both waves are found to have significant energy in the T-component, with a transverse-to-radial ratio of 0.35 ± 0.12 and 0.40 ± 0.14 for *SKS* and *SKKS*, respectively (Figure 3). There is a positive correlation between the two ratios (Figure 3c), suggesting that the two phases experienced same type of anisotropy. On the other hand, about 10% of the data show different behavior between the two waves (Figure 3d). For example, at station FFC (Flin Flon, Manitoba, Canada), *SKS* is observed to have significant energy on the T-component while $SKKS_T$ is almost negligible (Figure 4). The primary goal of this study is to find out whether this difference is significant and systematic.

3. Data Analysis

[9] The fast polarization direction, φ, and delay time, δt, are estimated by minimizing the energy on the T-component [*Silver and Chan*, 1991]. To investigate whether there is significant discrepancy in splitting between *SKS* and *SKKS*, we measured (φ, δt) with two types of anisotropic models: an isotropic or anisotropic lower mantle plus an anisotropic upper mantle. The first one predicts similar splitting between the two waves and needs only one set of (φ, δt) (hereafter referred to as 2-parameter model) to explain the data, while the second one requires two independent sets of

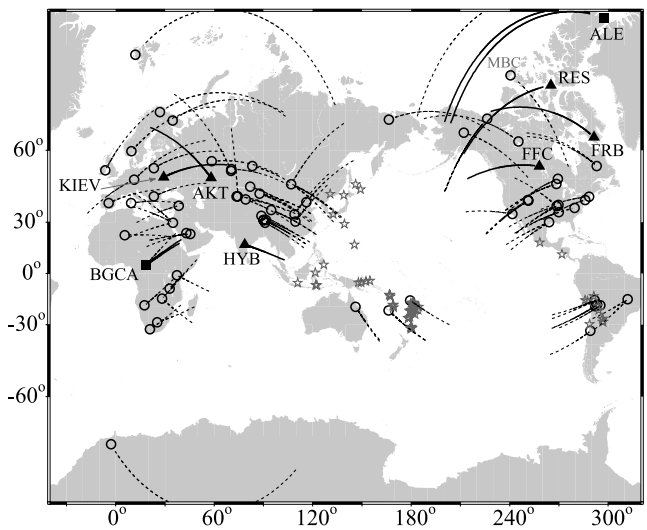

Figure 2. Map of the 76 stations (triangles, squares and circles) and events (stars) that are used in this study. Stations exhibiting significantly different splittings between *SKS* and *SKKS* are shown in solid triangles, while those shown similar ones are plotted with open circles. Both behaviors are found at stations ALE and BGCA, which are shown in solid squares. Lines indicate the receiver-side ray paths of *SKS* and *SKKS* in the lower mantle. The thick solid lines indicate the part of the lower mantle that shows either seismic anisotropy or anomalous dipping structures.

splitting parameters (4-parameter model) to match the *SKS* and *SKKS* waveforms. In both cases, we searched φ (defined as clockwise from the north direction) and δt in the range of 0°–180° and 1–4 s with increments of 1° and 0.05 s, respectively. For each pair of (φ, δt), we first calculated the predicted energy on the T-component for both *SKS* and *SKKS*. For the 2-parameter model, the fast polarization direction and splitting time are determined by minimizing the total energy of SKS_T and $SKKS_T$ (E_{K+KK}). For the 4-parameter model, the fast polarization direction and splitting time for *SKS* and *SKKS* are determined independently by searching the individual minimums (E_K and E_{KK}). We further calculated the variance of the data from the minimum energies of the two cases

$$\sigma_1^2 = E_{K+KK}^{\min}/(N-2)$$
$$\sigma_2^2 = \left(E_K^{\min} + E_{KK}^{\min}\right)/(N-4) \quad (1)$$

[*Menke*, 1989], where N is the total data points of the *SKS* and *SKKS* time series. It is usually assumed that E_{K+KK} and (E_K + E_{KK}) follow the *chi-squared distribution* with $\upsilon_1 = \upsilon - 2$ and $\upsilon_2 = \upsilon - 4$ degrees of freedom. Thus the ratio σ_1^2/σ_2^2, which is the relative "goodness" of the two models in terms of variance reduction, follows the *F distribution* with υ_1 and υ_2 degrees of freedom. A detailed explanation on how to calculate υ can be found in the appendix of *Silver and Chan* [1991]. It is found that for GSN broadband stations, 1 second of data corresponds roughly to 1 degree of freedom. We tested the significance in error improvement at 95% and 99% confidence levels.

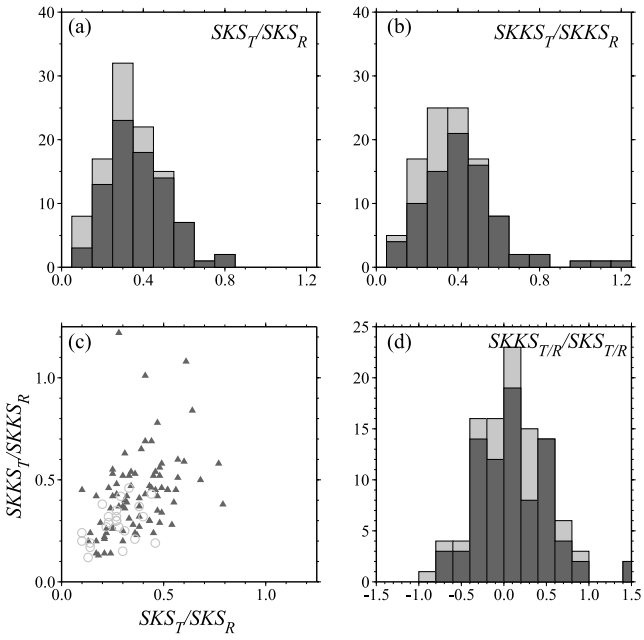

Figure 3. Histograms of the amplitude ratios SKS_T/SKS_R and $SKKS_T/SKKS_R$ are shown in (a) and (b), respectively. SKS_T or $SKKS_T$ with *SNR* >2.0 are shown in dark grey. (c) $SKKS_T/SKKS_R$ is plotted against SKS_T/SKS_R. The two exhibit a positive correlation with a few anomalous points. SKS_T or $SKKS_T$ with *SNR* >2.0 are shown in solid triangles; the others are plotted in open circles. (d) Histogram of the relative ratio of $SKKS_T/SKKS_R$ and SKS_T/SKS_R, plotted on logarithmic scale.

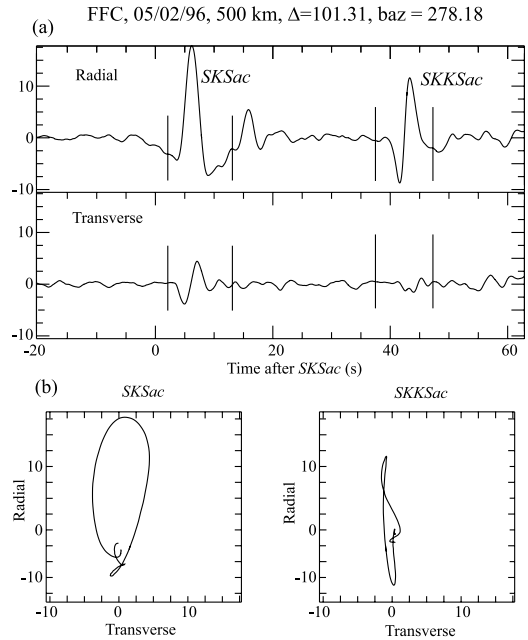

Figure 4. (a) An example of the radial and transverse components of *SKS*+*SKKS* seismogram observed at station FFC. Notice the large difference in the amplitude of SKS_T and $SKKS_T$. (b) Particle motions diagrams of *SKS* and *SKKS*.

[10] The above measurements are conducted mainly on the raw data. Most of the *SKS*/*SKKS* waveforms show a peak spectrum around 0.1–0.3 Hz. We have applied several different filtering, such as band pass filters 2–50s, 3–50s, 5–50s, 6–50s to the data. In general, measurements from the band pass filtered data are consistent with those from the raw data.

4. Results and Discussions

[11] Estimates of (φ, δt) based on the two models are listed in supplementary materials[1] with their 1σ errors. Measurements at the same or nearby stations from previous studies summarized by *Silver* [1996] are also listed for comparison. For most of the stations, our measurements are in good agreements with previous observations. Significant discrepancy is found at only very few stations, for example BLA (80.42W 37.21N). This discrepancy is probably due to azimuthal dependent splitting observed from medium with a depth varying anisotropy [e.g., *Silver and Savage*, 1994; *Rumpker and Silver*, 1998]. While the majority of the stations exhibit almost similar splitting pattern between the two waves, ten *SKS*+*SKKS* pairs recorded at eight stations (bold italic in supplement) are found to be better explained by the 4-parameter model at 95% confidence level. Three stations (BGCA, FFC, KIEV) further show a difference at 99% confidence level. In fact, the discrepancy in splitting can be confirmed from the raw data, as shown in the example in Figure 4. Usually one phase has significant energy while the other one is absent at the T-component. In some case, although the fast polarization directions derived from the two phases agree

[1]Auxiliary material is available at ftp://ftp.agu.org/apend/gl/2004GL021196.

with each other, but the delay times are very different (ALE, FRB). Among the eight stations we have two consistent observations at two stations but have only one measurement for the other six stations, partly because we have employed very strict criteria in selecting the data. For example, we have two additional events recorded at FFC which have slightly low $SKKS_R/SKS_R$ amplitude ratios ($\sim$0.4). We can also see the splitting difference between *SKS* and *SKKS* from these two events. Both come from roughly the same back azimuth with the event listed in the supplementary table and are characterized by a strong SKS_T and a weak $SKKS_T$, consistent with the observations shown in Figure 4. At two stations, mixed splitting results are found. The two phases show similar splitting pattern from some events, but different behaviors from events with different back azimuths (Figure 2).

[12] Among the eight stations, we found previous measurements at six stations. At ALE, RES and FRB those values are relatively consistent with our estimates derived from *SKKS* waves (see supplementary materials). At BGCA, we found null *SKS* splitting from two events that have back azimuths of 52° and 55°, suggesting that the fast direction is either parallel or perpendicular to the back azimuths. One of them agrees with $\varphi = 60$ as reported by *Vinnik et al.* [1992]. However, this value is quite different from our measurements based on a third event arriving from a slightly different back azimuth (42°). Consistent *SKS* and *SKKS* splittings are observed from this event. We obtained a null measurement from *SKS* splitting at HYB, in good agreement with the observation of *Barruol and Hoffmann* [1999]. Measurement of *SKKS* waveform, on the other hand, yields a splitting of $\sim$1s at the same station. We, however, noticed that the resulting slow direction ($-50° \pm 11°$) is very close to the back azimuth ($-72°$) and that large uncertainties exist at low frequency bands. We also should say that our results need further confirmation when more data are available.

[13] Four (ALE, RES, FRB and FFC) of the eight stations belong to the Canadian National Seismograph Network (CNSN). In fact another CNSN station, MBC (Figure 2), also shows some suggestive evidence of discrepancy between *SKS* and *SKKS* splitting. The other four stations seem to be randomly distributed. They are located in India (HYB), Kazakhstan (AKT), Ukraine (KIEV) and Central Africa (BGCA) (Figure 2).

[14] The epicentral distances of the ten pairs range from $\sim$100° to $\sim$115°. The separation of the *SKS* and *SKKS* ray paths at 660 km depth are about 80–100 km (Figure 1). The first Fresnel zone is about 140 km for an *SKS* or *SKKS* with a dominant period of 5 s at the same depth. The overlap of the first Fresnel zones of the two waves continues to depths around 1000 km. The observation that the *SKS* and *SKKS* recorded at the majority show the same splitting pattern thus suggests that contributions from transition zone and the uppermost mantle to *SKS*/*SKKS* splitting may be still possible. If the fast polarization directions of the lithosphere and underlying mantle lie within 45°, the resulting measurements of the apparent fast polarization and delay time may appear to be independent on events back azimuth [*Rumpker and Silver*, 1998], similar to the simple one-layer anisotropy model [*Silver and Chan*, 1991]. As for two-layer anisotropy model employed to explain complicated splitting feature at some stations, the deeper layer may extend to the uppermost lower mantle. In fact, recent experimental study [*Cordier et al.*, 2004] found that dislocation creep leading to seismic anisotropy can occur in this part of the lower mantle. On the other hand, our observations once again show that vast part of the lower mantle including the lowermost D'' region is azimuthally isotropic (or transversely isotropic). We, however, want to emphasize that the *SKS*/*SKKS* pair provide more compelling evidence than using deep earthquakes.

[15] The anomalous splitting patterns observed at the eight stations, on the other hand, suggest the presence of anomalous structures in the lower mantle. Such structures could be either anisotropic regions or dipping heterogeneous layers, and could be anywhere in the lower mantle from $\sim$1000 km to the CMB. Since they affect the two waves differently, the lateral scale of these structures must be less than the separation of the two paths, which is a few hundred kilometers.

[16] **Acknowledgments.** We thank the IRIS and Geoscope for providing the data. We thank G. Barruol and an anonymous reviewer for their constructive comments. This work was supported by the Department of Earth Science, Rice University.

References

Barruol, G., and R. Hoffmann (1999), Seismic anisotropy beneath the Geoscope stations from SKS splitting, *J. Geophys. Res.*, *104*, 10,757–10,774.

Cordier, P., T. Ungar, L. Zsoldos, and G. Tichy (2004), Dislocation creep in MgSiO3 perovskites at conditions of Earth's uppermost lower mantle, *Nature*, *428*, 837–840.

Hiramatsu, Y., M. Ando, and Y. Ishikawa (1997), ScS wave splitting of deep earthquakes around Japan, *Geophys. J. Int.*, *128*, 409–424.

Iidaka, T., and F. Niu (1998), Evidence for an anisotropic lower mantle beneath eastern Asia: Comparison of shear-wave splitting data of SKS and P660s, *Geophys. Res. Lett.*, *25*, 675–678.

Kennett, B. L. N., and E. R. Engdahl (1991), Travel times for global earthquake location and phase identification, *Geophys. J. Int.*, *105*, 429–465.

Mainprice, D., G. Barruol, and W. Ben Ismail (2000), The seismic anisotropy of the Earth's mantle: From single crystal to polycrystal, in *Earth's Deep Interior: Mineral Physics and Tomography From the Atomic to the Global Scale*, edited by S. I. Karato, pp. 237–264, AGU, Washington, D.C.

Meade, C., P. G. Silver, and S. Kaneshima (1995), Laboratory and seismological observations of lower mantle isotropy, *Geophys. Res. Lett.*, *22*, 1293–1296.

Menke, W. (1989), *Geophysical Data Analysis: Discrete Inverse Theory*, rev. ed., Elsevier, New York.

Nicolas, A., and N. I. Christensen (1987), Formation of anisotropy in upper mantle peridotites—A review, in *Composition, Structure and Dynamics of the Lithosphere-Asthenosphere System*, edited by K. Fuchs and C. Froidevaux, pp. 111–123, AGU, Washington, D.C.

Rumpker, G., and P. G. Silver (1998), Apparent shear-wave splitting parameters in the presence of vertically varying anisotropy, *Geophys. J. Int.*, *135*, 790–800.

Silver, P. G. (1996), Seismic anisotropy beneath the continents: Probing the depths of geology, *Annu. Rev. Earth Planet. Sci.*, *24*, 385–432.

Silver, P. G., and W. W. Chan (1991), Shear wave splitting and subcontinental mantle deformation, *J. Geophys. Res.*, *96*, 16,429–16,454.

Silver, P. G., and M. K. Savage (1994), The interpretation of shear-wave splitting parameters in the presence of two anisotropic layers, *Geophys. J. Int.*, *119*, 949–963.

Vinnik, L. P., and J. P. Montagner (1996), Shear wave splitting in the mantle Ps phase, *Geophys. Res. Lett.*, *24*, 2449–2452.

Vinnik, L. P., L. I. Makeyeva, A. Milev, and Y. Usenko (1992), Global patterns of azimuthal anisotropy and deformation in the continental mantle, *Geophys. J. Int.*, *111*, 433–447.

Wookey, J., J.-M. Kendall, and G. Barruol (2002), Mid-mantle deformation inferred from seismic anisotropy, *Nature*, *415*, 777–780.

Yeganeh-Haeri, A. (1994), Synthesis and re-investigation of elastic properties of single-crystal magnesium silicate perovskite, *Phys. Earth Planet. Inter.*, *87*, 111–121.

F. Niu and A. M. Perez, Department of Earth Science, Rice University, 6100 Main Street, Houston, TX 77005, USA. (niu@rice.edu; anisa@rice.edu)